

# TubeR: Tube-Transformer for Action Detection

Jiaojiao Zhao<sup>1\*</sup>Arthur Li<sup>2</sup>Chunhui Liu<sup>2</sup>Shuai Bing<sup>2</sup>Hao Chen<sup>2</sup>Cees G.M. Snoek<sup>1</sup><sup>1</sup>University of Amsterdam

{j.zhao3, cgmsnoek}@uva.nl

Joseph Tighe<sup>2</sup><sup>2</sup>Amazon Web Service

{xxnl, chunhliu, bshuai, hxen, tighej}@amazon.com

## Abstract

In this paper, we propose TubeR: the first transformer based network for end-to-end action detection, with an encoder and decoder optimized for modeling action tubes with variable lengths and aspect ratios. TubeR does not rely on hand-designed tube structures, automatically links predicted action boxes over time and learns a set of tube queries related to actions. By learning action tube embeddings, TubeR predicts more precise action tubes with flexible spatial and temporal extents. Our experiments demonstrate TubeR achieves state-of-the-art among single-stream methods on UCF101-24 and J-HMDB. TubeR outperforms existing one-model methods on AVA and is even competitive with the two-model methods. Moreover, we observe TubeR has the potential on tracking actors with different actions, which will foster future research in long-range video understanding.

## 1 Introduction

This paper tackles the problem of spatio-temporal action detection in videos, which plays a central role in advanced video search engines, surveillance systems, and self-driving cars. The task requires to localize all the people in the frame and predict their action labels. Successful existing methods, e.g., [9, 29, 33, 41] rely on carefully-designed anchors or a huge number of sliding windows to first localize actors and then recognizing their actions for a single frame. Although they rely on ‘one-model’ to jointly train the two tasks, the detection results are heavily dependent on the anchors. Recently, both Jiang et al. [16] and Feichtenhofer et al. [7] show even better performance with ‘two-model’ designs. The first model is an off-the-shelf person detector providing a region-of-interest (ROI) [11] on a keyframe. They duplicate the detected boxes over time to form a cuboid. Features are then

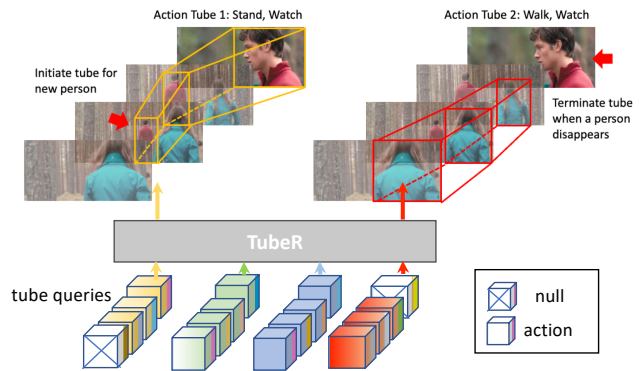


Figure 1: **TubeR automatically generates action tubes** with a flexible spatial and temporal extent by a set of learned tube queries. TubeR does not require pre-defined anchors and post-processing.

pooled across these cuboids using a second model to recognize the actions of the corresponding actors. We consider the search through the huge anchor spaces of one-model methods and the extra detector required for person localization of two-model methods inefficient and unsatisfying. In this paper, we propose the Tube-Transformer (TubeR) framework for generating action tubelets that simultaneously locate and recognize actions, all in a single model. Instead of pre-designing anchors, TubeR learns a set of tube queries related to action positions from spatio-temporal video features (as shown in Figure 1).

Vaswani et al. [36] proposed the transformer for machine translation (a 1D sequence task), and soon after it became the most popular backbone on sequence-to-sequence tasks, e.g., [18, 20, 34]. Recently, it has also demonstrated impressive advances in object detection [1, 46] and image classification [3, 43] (a 2D image task). Self-attention enables transformers to selectively attend to the most relevant information and relationships. This naturally inspires us to explore how to model more complicated information along spatio-temporal space (in 3D video tasks) by using the transformer.

\*This work was done during internship at Amazon.

Encouraged by the success of DETR [1] and Deformable-DETR [46] for object detection, we are the first to target the challenging task of human action detection in video with a transformer architecture. Rather than focusing on the actor only in a single frame [10,33], or cuboid [7,16], our intuition is that when detecting actions it is beneficial to consider the spatio-temporal space surrounding an actor. The transformer allows each 3D position to attend to all the other 3D positions in a video clip, which is essential for modeling the action relations in video and detecting action tubes along the spatio-temporal space.

We make two technical contributions. First, we propose TubeR, a tube-transformer with an encoder and decoder optimized for modeling action tubes with variable lengths and aspect ratios. TubeR does not rely on hand-designed tube structures and learns a set of tube queries related to actions. Second, we design spatial→temporal multi-head attention to model tube queries spatially and temporally. The transformer decoder is able to utilize the learned tube queries for activity-specific spatio-temporal feature querying. Our experiments demonstrate TubeR outperforms existing single-stream approaches on UCF101-24 and J-HMDB, obtains best performance among one-model methods on AVA and is competitive with the two-model state-of-the-art.

## 2 Related Work

**ConvNet for action detection.** Spatio-temporal human action detection [5,12,25,29,37,44] in video has made considerable progress with the rise of deep convolutional neural networks(ConvNets). Most existing methods, e.g., [12,17,21,25,41,42] using ConvNets are anchor-based. Earlier, Gkioxari and Malik [12] directly built upon a 2D object detection framework for detecting actions on single frames before linking the box detections into action tubes. To compensate for the lack of temporal information, optical flow is applied by [25,29,45]. Hou et al. [14] extend 2D box anchors to 3D tube anchors for directly locating and predicting action tubes. Kalogeiton et al. [17] exploit temporal continuity by taking as many as six frames as input for their 2D detector. Li et al. [22] developed an anchor-free detector based on CenterNet [4] by treating an action instance as a trajectory of moving points. Recently, 3D convolutional networks are preferred for extracting spatio-temporal features, which has proven useful for recognizing actions [2,7,38,39].

As a large dataset for action detection, AVA [13] has become popular. Since AVA only has keyframe annotations, Gu et al. [13] leverage two separated models for detecting actors and recognizing actions on keyframes. The state-of-the-art on AVA [6,7,33,44] follows this regime for utilizing spatio-temporal features to recognize actions. However, this cuboid design ignores the spatial displacements of an actor over time, which introduces noise for action recognition.

Continuing this line of work, Feichtenhofer et al. [6,7] use an off-the-shelf person detector to locate actors before recognizing the actions. The action detection performance is improved but introduces a non-reversible dependence on the person detector. Yang et al. [41] develop a progressive learning to refine tube proposals for generating tubes on a clip. All the methods require well-designed anchors or a huge numbers of sliding windows to cover all possible actions in a frame or video. Our proposed TubeR is different, as it learns a set of tube queries related to actions and simultaneously outputs the spatio-temporal location of an action and its corresponding class labels.

**Attention for Action Analysis.** Self-attention mechanisms allows the transformer to selectively attend on the most relevant pieces of information and relationships in a sequence. Previously, Girdhar et al. [10] utilized a transformer-decoder for helping action classification and Pramono et al. [26] designed a hierarchical self-attention for improving action localization accuracy. Both methods still need region proposal networks to generate many actor proposals. Thus, these methods are still Faster-rcnn style detectors. Gavrilyuk et al. [8] use a transformer-encoder for group activity recognition. Recently, DETR [1,46] applied a transformer encoder-decoder architecture for a concise object detection without any pre-designed anchors or post-processing. Our TubeR also no longer needs pre-designed anchors or post-processing and introduces a new transformer framework targeting on the challenging task of action detection in videos.

## 3 Action Detection by TubeR

We now present our TubeR system that simultaneously detects and links actors and predicts their actions, without the need for anchors or separate person detectors. Given a video clip  $I \in \mathbb{R}^{T_0 \times H_0 \times W_0 \times C}$ , where  $T_0, H_0, W_0, C$  denote the number of frames, height, width and colour channels respectively, a 3D network is applied as a backbone to generate low-spatial-resolution activation maps  $F \in \mathbb{R}^{T_0 \times H \times W \times C}$ ,  $H < H_0, W < W_0$ , while keeping the original temporal dimension. We introduce an encoder with *3D positional encoding* for modeling the spatio-temporal features and a *tube-decoder* that directly predicts a set of action tubes (eq. 1), each representing a person through time and the actions they are performing. The key components of TubeR are illustrated in Figure 2.

We define an action tube  $y$  with multiple action labels  $c$  across a video clip with length  $T_0$  as:

$$\begin{aligned} y &= (c, B), \\ B &= [b_1, \dots, b_{T_0}]. \end{aligned} \tag{1}$$

Here,  $B$  is a list of bounding boxes per frame.  $b_t \in [0, 1]^4$  represents the action’s spatial location on the  $t$ -th frame. We

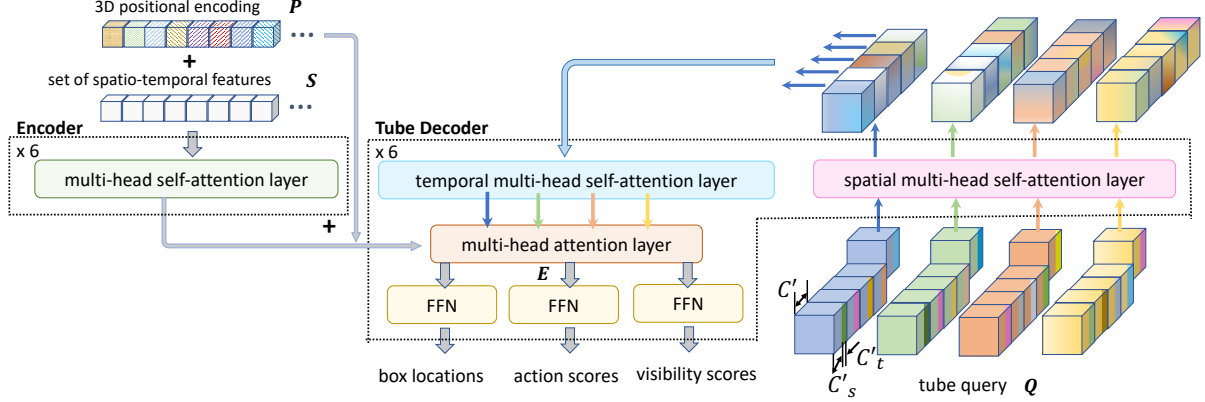


Figure 2: **TubeR encoder-decoder structure.** Both encoder and tube decoder contain six stacked modules. We only show the key components in the encoder and decoder modules. Encoder models the spatio-temporal features from backbone by multiple multi-head self-attention layers (see Section 3.1). The decoder transforms a set of tube queries and finally predicts action tubes. All box queries in a tube query share the same set of parameters for the first  $C'_s$  channels (representing the visual similarity in the tube), and allow each to have independent parameters for the last  $C'_t$  channels (to capture changes over time). Then we utilize a spatial multi-head self-attention layer to model the relations between box queries within a frame and then adopt a temporal multi-head self-attention layer to model the relations between box queries within a tube. Following, a multi-head attention layer is applied to learn the relations between tube queries and encoded features. Finally, TubeR outputs box location, action scores and visibility scores for each box in a tube (see Section 3.2).

use  $t$  as the index of the frame. It is a tuple of bounding box center coordinates and its height and width relative to the frame size.  $b_t$  can be  $\emptyset$  when the action or actor is no longer visible in the  $t$ -th frame. We use  $c = [c_1, \dots, c_M]$ ,  $c_j \in \{0, 1\}$ ,  $j \in \{1, \dots, M\}$  to represent the action label of the tube from a pool of  $M$  possible action labels. Here  $c_j=1$  indicates that the tube has an action class label  $j$ .

### 3.1 TubeR Encoder

**Self-attention layers.** The self-attention mechanism is a key component of the transformer. A vanilla self-attention layer [36] operates by having each position attend over all positions in a sequence. Specifically, the self-attention layer first maps its inputs to a query  $X_Q$ , a key  $X_K$  and a value  $X_V$  in a shared embedding space using linear projections. Here  $X_Q$  and  $X_K$  have the same feature dimension  $d_k$ , while  $X_V$  has the feature dimension  $d_v$ . The output for a query is computed as an attention weighted sum of values  $X_V$ , where the attention weights are obtained from the dot product of the query  $X_Q$  with keys  $X_K$ .

$$\text{Self-attention}(X_Q, X_K, X_V) = \text{softmax}\left(\frac{X_Q X_K^T}{\sqrt{d_k}}\right) X_V. \quad (2)$$

A multi-head self-attention layer [36] is designed for allowing a model to jointly attend to information from different representation subspaces at different positions. It runs through a self-attention mechanism several times in parallel. The independent attention outputs are then concatenated and linearly transformed into the expected dimension.

**Encoder.** Our TubeR encoder models global context in an input video clip. It stacks several blocks, with each of the block made up of a multi-head self-attention layer, several normalization layers and a feed forward network (FFN). Different from the vanilla transformer encoder, the TubeR encoder is designed for processing information in the 3D spatio-temporal space. Taking the video features  $F$  from a backbone, we first project  $F$  to  $F' \in \mathbb{R}^{T_0 \times H \times W \times C'}$  with a low feature dimension  $C'$ . We then flatten spatial temporal dimensions of  $F'$  to one dimension getting  $S$  with shape  $L \times C'$ ,  $L = T_0 \times H \times W$ . With the self-attention mechanisms, the tube encoder globally models the relations among all vectors in  $S$ .

**3D positional encoding.** Transformers require the positional encoding equipped to the input of each attention layer [36]. We propose a 3D positional encoding  $P \in \mathbb{R}^{L \times C'}$  with the length  $L$  which can be added element-wise to the transformer input  $S$ . To represent a specific 3D position, we use three sets of sinusoidal positional encodings [36],  $P_W \in \mathbb{R}^{W \times C'_W}$ ,  $P_H \in \mathbb{R}^{H \times C'_H}$ ,  $P_T \in \mathbb{R}^{T_0 \times C'_T}$ , to encode the index along *width*, *height*, and *time* dimensions of  $F'$ , where  $C'_W + C'_H + C'_T = C'$ . Specifically, along the width dimension, for the token position  $w$  and the channel  $d_W$ , the positional encoding is:

$$P_{W(w, d_W)} = \begin{cases} \sin\left(\frac{w}{10,000^{2d_W/C'_W}}\right), & \text{for } d_W = 2k \\ \cos\left(\frac{w}{10,000^{2d_W/C'_W}}\right), & \text{for } d_W = 2k + 1 \end{cases},$$

where  $w = \{1, \dots, W\}$ ,  $d_W = \{1, \dots, C'_W\}$ ,  $k = \{1, \dots, \lfloor C'_W/2 \rfloor\}$ . Similarly, we obtain  $P_{H(h, d_H)}$  and  $P_{T(t, d_T)}$ . A 3D position  $(t, h, w)$  on  $F'$  corresponds

to a position  $thw$  in  $S$ . A unique positional encoding  $P_{(thw)} = [P_{T(t)}, P_H(h), P_W(w)]$ .  $[\cdot]$  represents concatenation along the channel dimension.

### 3.2 TubeR Decoder

In vanilla transformers, the decoder is structured with  $N$  fixed outputs. Starting with a set of  $N$  learned query embeddings, each decoder block uses these as queries applied to the encoder feature. Multiple decoder blocks are chained together to refine the final  $N$  prediction embeddings. The input embeddings are parameters learned during training and the output embeddings are feature representations that are used for the final prediction.

To directly generate action tubes, we define a set of  $N$  tube embeddings which we call *tube queries*. To model the tube queries spatially and temporally, we design a spatial multi-head self-attention layer and a temporal multi-head self-attention layer as shown in Figure 2. Then, a multi-head attention layer is applied to model the relations between the tube queries and the encoded video features. We describe more details below.

**Tube query.** Directly detecting tubes is quite challenging as the tube space along the spatio-temporal dimension is huge compared to the single frame bounding box space. Thinking about Faster-rcnn [27] for object detection, for a feature map with spatial size  $H' \times W'$ , each position requires  $K (=9)$  anchors. There are in total  $KH'W'$  anchors. For a tube across  $T_0$  frames, it would require  $(KH'W')^{T_0}$  anchors to maintain the same sampling in space-time. To alleviate the tube space, most of these methods adopt 3D cuboids to approximate tubes by ignoring the spatial action displacements, which can introduce noise when recognizing actions or form a polluted action tube with multiple actions. Rather than manually designing a large number of tube anchors, we utilize our transformer to learn a set of tube query embeddings  $Q = \{Q_1, \dots, Q_N\}$  driven by the data. Following eq. 1 a *tube query*  $Q_i = \{q_{i,1}, \dots, q_{i,T_0}\}$  contains  $T_0$  *box queries*  $q_{i,t} \in \mathbb{R}^{C'}$ . Here  $i = \{1, \dots, N\}$  indicates the index of the tube queries. By modeling the relations between each tube query and the global spatio-temporal features for detecting actions, our model learns tube queries related to actions and predicts action boxes for each frame. To generate a tube, we initialize the box embeddings such that for each tube query, the box queries are close together in feature space but not identical. Our idea here is that a tube should be made up of a set of boxes that while similar in appearance and spatial extent, do change over time. We achieve this by having all box queries in a tube query share the same set of parameters for the first  $C'_s$  channels (representing the visual similarity in the tube), and allow each to have independent parameters for the last  $C'_t$  channels (to capture changes over time) such that  $C'_s + C'_t = C'$ . We keep  $C'_t$  smaller than  $C'_s$  to guide the

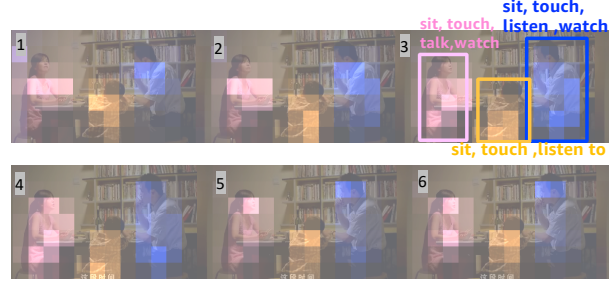


Figure 3: **What the TubeR decoder learns.** A query attends to the same actor across all frames. On the keyframe, attention maps cover the whole actor for locating actors. And on other frames, the attention selectively focuses on faces, arms for recognizing actions.

tube to focus on the same person.

**Multi-head self-attention layers in TubeR.** In our TubeR, the multi-head self-attention layer is applied for exploring the relations between tube queries spatially and temporally. Specifically, we use two multi-head self-attention layers to model the relations by a spatial  $\rightarrow$  temporal configuration. First we have our *spatial multi-head self-attention layer* (Figure 2) that processes the spatial relations between box queries within a frame, i.e.  $\{q_{1,t}, \dots, q_{N,t}\}$ . The intuition of this layer is that recognizing actions really depends on the interactions between actors, or between actors and objects in the same frame. Next we have our temporal multi-head self-attention layer that models the relationships between queries in the same tube across time i.e.  $\{q_{i,1}, \dots, q_{i,T_0}\}$ . This layer facilitates a TubeR query to track actors and generate action tubes that focus on single actors instead of a fixed area in the frame. We visualize the query attention maps in Figure 3. On the keyframe, the attention maps cover more on the whole actor which we believe is useful for locating actors. And on other frames, we find the attention selectively focus more on faces, arms which are critical for recognizing actions. It observed one query attends to the same actor across the frames, which helps to generate a tube.

**Decision layers.** Our tube decoder finally predicts  $N$  tubes  $\hat{Y} = \{\hat{y}_i\}$ .

$$\begin{aligned} \hat{y}_i &= (\hat{c}_i, \hat{B}_i), \\ \hat{B}_i &= \{\hat{b}_{i,1}, \dots, \hat{b}_{i,T_0}\}. \end{aligned} \quad (3)$$

Each  $\hat{y}_i$  contains  $T_0$  box predictions ( $\hat{B}_i$ ) and a vector of classification scores for each action category ( $\hat{c}_i$ ). We utilize a feed-forward network (FFN) to independently decode the coordinates of a box  $\hat{b}_{i,t} \in [0, 1]^4$  from the corresponding output embedding  $e_{i,t}$ .

$$\hat{b}_{i,t} = \text{FFN}_{\text{box}}(e_{i,t}). \quad (4)$$

To remove non-action boxes, we apply an FFN for deciding whether a box prediction visibly depicts the actor performing

the action(s) of the tube. This allows our TubeR to generate action tubes of different lengths. The probability of a predicted box  $\hat{b}_{i,t}$  being visible is:

$$\hat{s}_{i,t} = \text{FFN}_{\text{visibility}}(e_{i,t}). \quad (5)$$

For action classification, the representation of a box query is an average of all output embeddings in the tube so that all box queries in a tube share the same representation and produce same action scores. The representation is fed into a FFN. The probabilities of the  $M$  action classes  $\hat{c}_i \in [0, 1]^M$  for a predicted box  $\hat{b}_i$  estimated as:

$$\hat{p}_{i,j} = \text{FFN}_{\text{class}}(\text{Average}([e_{i,1}, \dots, e_{i,t}])). \quad (6)$$

### 3.3 Tube Matcher

Generally, for datasets with per-frame annotations, e.g. UCF101-24 and J-HMDB, we first construct ground-truth tubes. To calculate our losses during TubeR training, we need to match the  $N$  predictions  $\hat{Y}$  to a set of ground-truth tubes  $Y$ . We set the number of predictions  $N$  to be larger than the possible number of ground-truth tubes. A ground-truth tube  $y_i = (c_i, B_i)$ ,  $B_i = \{b_{i,1}, \dots, b_{i,T_0}\}$  with action labels  $c_i = [c_{i,1}, \dots, c_{i,M}]$  is an action tube defined in eq. 1. For the dataset AVA, which only has keyframe annotations, we perform matching only on the keyframes in a clip.

In order to remove duplicates and find unique matches between predictions and ground-truth, TubeR builds upon the Hungarian matching algorithm from [1, 19, 32]. To adapt this matching algorithm to our tube action prediction framework, we introduce a per-frame on-off mechanism to allow tubes to match to just a portion of the key frames without penalizing for spurious detection on the other key frames. We minimize the sum of pair-wise matching costs between predictions and ground-truth on the  $t$ -th frame by searching for an optimal permutation of  $N$  elements  $\delta_t \in \mathfrak{G}_N$ :

$$\hat{\delta}_t = \arg \min_{\delta_t \in \mathfrak{G}_N} \sum_{i=1}^N \mathcal{L}_{\text{match}}(b_{i,t}, \hat{b}_{\delta_t(i),t}). \quad (7)$$

where  $\mathfrak{G}_N$  is a set of all the permutations of  $N$  and  $\delta_t(i)$  is the index of the matched prediction for the  $i$ -th ground-truth box on the  $t$ -th frame. If the  $t$ -th frame has no annotations, we skip it. The matching cost between the ground-truth box  $b_{i,t}$  and the prediction  $\hat{b}_{\delta_t(i),t}$  is decided by the matching action class label and bounding boxes. Specifically,  $\mathcal{L}_{\text{match}}(b_{i,t}, \hat{b}_{\delta_t(i),t})$  w.r.t. action tubes is:

$$\begin{aligned} \mathcal{L}_{\text{match}}(b_{i,t}, \hat{b}_{\delta_t(i),t}) = & - \sum_{j=1}^M \hat{s}_{\delta_t(i),t} * \mathbb{1}_{(c_{i,j}=1)} \hat{p}_{\delta_t(i),j} \\ & + \mathbb{1}_{(c \neq \emptyset)} \mathcal{L}_{\text{box}}(b_{i,t}, \hat{b}_{\delta_t(i),t}), \end{aligned} \quad (8)$$

where  $M$  is the total number of action classes. We use a weighted sum of the  $\ell_1$  loss and the generalized IoU [28] loss to measure a pairwise box match:

$$\mathcal{L}_{\text{box}}(b, \hat{b}) = \lambda_{\ell_1} \|b - \hat{b}\|_1 + \lambda_{\text{iou}} \mathcal{L}_{\text{iou}}(b, \hat{b}), \quad (9)$$

$$\mathcal{L}_{\text{iou}}(b, \hat{b}) = 1 - \left( \frac{|b \cap \hat{b}|}{|b \cup \hat{b}|} - \frac{|B(b, \hat{b}) \setminus b \cup \hat{b}|}{B(b, \hat{b})} \right). \quad (10)$$

Here we simply use  $b$  and  $\hat{b}$  to represent any two boxes.  $\lambda_{\ell_1}$  and  $\lambda_{\text{iou}}$  are hyperparameters.  $|\cdot|$  is an operation for computing area and  $B(b, \hat{b})$  represents the largest box containing  $b$  and  $\hat{b}$ .

**Losses** We utilize three losses: an action classification loss, a box matching loss and a visibility loss to train TubeR. For UCF101-24 and J-HMDB, losses are calculated on each frame with annotation in a tube. For AVA, losses are only calculated on annotated keyframes. The total loss is a linear combination of the three losses:

$$\begin{aligned} \mathcal{L}(Y, \hat{Y}) = & \sum_{t=1}^{T_0} \sum_{i=1}^N [\lambda_1 \mathcal{L}_{\text{visibility}}(b_{i,t}, \hat{b}_{\delta_t(i),t}) \\ & + \lambda_2 \mathbb{1}_{(b_{i,t} \neq \emptyset)} \mathcal{L}_{\text{class}}(b_{i,t}, \hat{b}_{\delta_t(i),t}) \\ & + \lambda_3 \mathbb{1}_{(b_{i,t} \neq \emptyset)} \mathcal{L}_{\text{box}}(b_{i,t}, \hat{b}_{\delta_t(i),t})]. \end{aligned} \quad (11)$$

$$\begin{aligned} \mathcal{L}_{\text{visibility}}(b_{i,t}, \hat{b}_{\delta_t(i),t}) = & \mathbb{1}_{(b_{i,t} \neq \emptyset)} \log \hat{s}_{\delta_t(i),t} \\ & + \mathbb{1}_{(b_{i,t} = \emptyset)} \log(1 - \hat{s}_{\delta_t(i),t}), \end{aligned} \quad (12)$$

$$\begin{aligned} \mathcal{L}_{\text{class}}(b_{i,t}, \hat{b}_{\delta_t(i),t}) = & - \sum_{j=1}^M \log \hat{s}_{\delta_t(i),t} * [c_j \log \hat{p}_{\delta_t(i),j} \\ & + (1 - c_j) \log \hat{p}_{\delta_t(i),j}]. \end{aligned} \quad (13)$$

## 4 Experiments

### 4.1 Settings

**Datasets.** We conduct our experiments on three datasets. **UCF101-24** [31] is a subset of UCF101. It contains 24 sport classes in 3207 untrimmed videos. We use the revised annotations for UCF101-24 from [29] and only report the performance on the split-1.

**J-HMDB** [15] contains 21 action categories in 928 trimmed videos. We report the average results on three splits. For both datasets, we report video- $mAP$  at high IoU thresholds 0.5 and 0.5:0.95.

**AVA** [13] targets spatio-temporal action detection. It has 437

	UCF101-24		J-HMDB	
	0.50	0.50:0.95	0.50	0.50:0.95
<b>single-stream (RGB)</b>				
Kalogeiton et al. [17]	41.8	18.5	60.0	34.0
Song et al. [30]	45.0	19.4	64.5	35.1
Zhao et al. [45]	45.6	20.2	63.6	38.0
Li et al. [22]	51.0	<b>26.5</b>	-	-
<b>TubeR,TPN</b>	<b>52.0</b>	25.2	<b>79.5</b>	<b>58.0</b>
<b>two-stream (RGB+FLOW)</b>				
Kalogeiton et al. [17]	49.2	23.4	73.7	44.8
Song et al. [30]	52.9	24.1	73.4	44.8
Zhao et al. [45]	50.3	24.4	74.7	45.0
Li et al. [22]	53.8	28.3	77.2	59.1

Table 1: **Comparison on UCF101-24 and J-HMDB** with video- $mAP$ . Only taking RGB as inputs, TubeR with backbone TPN [40] performs much better on J-HMDB and is comparable to state-of-the-art on UCF101-24 among single-stream methods. Without using optical flow, TubeR even outperforms most two-stream methods on both datasets.

videos with 211k training and 57k validation keyframes sampled one per second. Annotations are provided per keyframe. We follow the standard protocol of evaluating on 60 classes [13] by  $mAP$  with a frame-level IoU threshold of 0.5 as the metric. In addition, we also evaluate person detection by TubeR and report the person  $mAP@IoU=0.5$ .

**Training and inference.** We experiment with several 3D network backbones pretrained on the Kinetics-400 action classification task for extracting video features. For training, we take an input video clip of 9 frames in lengths by sampling every 4th frame, which covers 36 frames in the original video. We first resize each video frame with the short side to 332 and randomly crop them with the short side 300. We set the size of the prediction set  $N$  equal to 15. We set the number of channels for a box query  $C'=256$ . As actions change smoothly over time, we used less channels to represent temporal changes. Thus, we set the spatial channels  $C'_s=224$  and temporal channels  $C'_t=32$ . If we set  $C'_t=16$ , the  $mAP$  drops slightly ( $< 0.5$ ). With  $C'_t=64$ , the  $mAP$  drops more than 1. The initial learning rate for the backbone and the transformer are  $1 \times 10^{-5}$  and  $1 \times 10^{-4}$  respectively. For UCF101-24 and J-HMDB, We train our network with an AdamW [24] optimizer for 30 epochs with a learning rate dropped by a factor of 10 after 20 epochs. For AVA, we train 120 epochs with a learning rate dropped by a factor of 10 after 100 epochs. For inference, video clips are resized on 300 at the short side for full resolution test.

## 4.2 Comparisons to the State-of-the-art

We only consider RGB inputs for TubeR as the optical flow requires extra computation. Seen from Table 1, Tu-

	flow	pretrained	action $mAP$
<b>one-model</b>			
I3D [13]		K400	14.5
I3D [13]	✓	K400	15.6
ACRN,S3D [33]	✓	K400	17.4
STEP,I3D [41]		K400+AVA	18.6
I3D [9]		K600	21.9
<b>TubeR,SlowFastR50</b>		K400	<b>22.8</b>
<b>two-model</b>			
SlowOnlyR50+Faster-rcnn [7]		K400	19.0
ATR,R50+NL [16]		K400	20.0
SlowFastR50+Faster-rcnn [7]		K400	24.2
Tr+I3D [10]		K400	24.9
X3D XL+Faster-rcnn [6]		K400	26.1
SlowFastR101-NL+Faster-rcnn [7]		K600	<b>28.2</b>
<b>TubeR+SlowFastR101-NL</b>		K600	27.8

Table 2: **State-of-the-art comparison on AVA** with frame- $mAP@IoU=0.5$ . TubeR achieves highest  $mAP$  among one-model methods and is competitive among two-model works.

beR with TPN [40] as backbone outperforms most single-stream methods and is even comparable to the state-of-the-art two-stream method on UCF101-24. On J-HMDB, TubeR achieves the best performance with a large margin compared to existing single-stream methods. Without optical flow, TubeR still obtains the state-of-the-art with video- $mAP@IoU=0.5$ .

We compare with previous one-model methods and two-model methods on AVA in Table 2. Among one-model methods, which only apply one backbone for action localization and recognition, TubeR with a SlowFastR50 backbone outperforms all the competitors. Two-model solutions benefit from using an action classification backbone pre-trained on additional datasets. To have a fair comparison with these two-model solutions, we add a slowfast [7] branch to our TubeR and use our TubeR detection results at keyframes to pool spatio-temporal feature from slowfast backbone. Doing so, we are able to achieve comparable action detection performance. It is important to note: 1) the best two-model solutions decompose the action detection into detection then classification problem, which doesn't consider the feature-wise association of two tasks, and 2) the two-model solutions are considerably slower. Our proposed TubeR does not rely on a separate detection network and thus can leverage features for both tasks while remaining computationally efficient for inference: our TubeR runs at 20 fps on a Tesla v100 GPU with spatial input size  $224 \times 224$ .

## 4.3 Ablation Study

For our ablation study, we train our network with smaller input sizes to allow for faster training. The short side of frames are resized to 256 and randomly cropped to 224 for

	enc.	emb.	<i>a-mAP</i>	<i>p-mAP</i>
frame	2D	box	19.1	92.8
frame	3D	box	19.5	95.0
tube	3D	tube	20.0	94.4

Table 3: **Tube detection vs. single frame detection.** TubeR for tube detection gains improvements on action *mAP*. enc. denotes positional encoding and emb. denotes query embedding.

self-attention	<i>a-mAP</i>	<i>p-mAP</i>
temporal	17.9	93.2
spatio-temporal	18.9	93.3
spatial→temporal	19.6	94.1

Table 4: **Multi-head self-attention layers.** Three ways to generate action tubes. Modeling spatial before temporal relations is best.

training. For showing more complicated cases, all ablation studies are conducted on AVA, as UCF101-24 and J-HMDB are considered easier. 3D-Resnet50 is used as the backbone. *a-mAP* denotes action *mAP* and *p-mAP* denotes person *mAP*.

**Effectiveness and efficiency.** We first compare with a two-model method which adopts a Faster-rcnn person detector and a 3D-Resnet50 network for recognizing actions [7]. The two-model method achieves action *mAP* 19.0%. As a one-model method, TubeR simultaneously predicts action boxes and labels gains 20% on action *mAP*. From the comparison on the *fps* of inference, TubeR (20 fps) is four times faster than the two-model method (5 fps). For training, as TubeR is based on transformers and jointly optimizes detection and classification, it needs 120 epochs to converge. As reported in [7], Slowfast trains the action classification on AVA for 68 epochs, but it does not report the training time for the off-line person detector (pretrained on ImageNet and COCO and finetuned on AVA).

**Tube detection vs. single frame detection.** TubeR is developed for end-to-end detection of a tube in a clip, but is also easily adapted to detect actions on a single frame. We have two options for this purpose. For the first option, we apply temporal pooling to aggregate the spatio-temporal features for a keyframe on the center position of an input clip. Our transformer takes as input the aggregated features and predicts the action locations and labels for the keyframe. Only 2D positional encoding and box query embeddings are needed here. The second option still keeps the temporal dimension of the video features  $F$ . Our transformer takes as input the spatio-temporal features of the whole input clip, but is expected to detect the actions only for the keyframe. This way, our transformer also processes the information

multi-head attention	<i>a-mAP</i>	<i>p-mAP</i>
long band features	18.9	93.3
short band features	20.0	94.4

Table 5: **Multi-head attention layers.** Applying the multi-head attention layer in the short band variant is best.

backbone	depth	<i>Acc %</i>	<i>a-mAP</i>	<i>p-mAP</i>
I3D	R50	76.1	20.0	94.4
I3D	R101	77.0	21.5	94.5
TPN [40]	R50	77.3	21.7	95.0
TPN [40]	R101	78.1	22.3	95.0

Table 6: **Generalization ability.** Adopting better pretrained backbone models on action classification (Kinetics-400) leads to better action detection.

along time, which may help recognize actions. As seen from Table 3, comparing the results on single frame detection, our TubeR is able to process spatio-temporal features with the help of 3D positional encoding and achieves better results for action and person. With our tube design, action detection is further boosted but the person detector drops a little. It is reasonable as detecting persons on a single frame is easier but recognizing actions requires video context.

**Multi-head self-attention layers.** Besides the spatial→temporal configuration, we also try to use only a single multi-head self-attention layer to model tube queries. One configuration models relations between box queries within and across frames, i.e.,  $Q^{(NT_0) \times C'}$ . We refer to this as the spatio-temporal configuration. It increases the tube search space by modeling relations between each pair of single box queries. It may introduce noise for generating tubes. Another configuration is first merging box queries of a tube into one embedding and then modeling the relations between the merged tube embeddings, i.e.  $Q^{N \times (T_0 C')}$ . We refer to this as the temporal configuration. Temporal configuration searches a much smaller tube space and may lose key information for recognizing actions. We compare the three configurations for the TubeR decoder to generate action tubes. We report the action *mAP* and person *mAP* in Table 4. It is observed that the (spatial→temporal) configuration better tracks an actor and improves action detection by first modeling spatial relations and then temporal relations between each tube.

**Multi-head attention layers.** Moreover, we study two configurations of applying the multi-head attention layer in Table 5. The first one decodes each box query from the whole encoded video features, which we call *long band features*. This configuration may introduce false positive detections when a video clip has scene cuts (shown in Figure 5). The

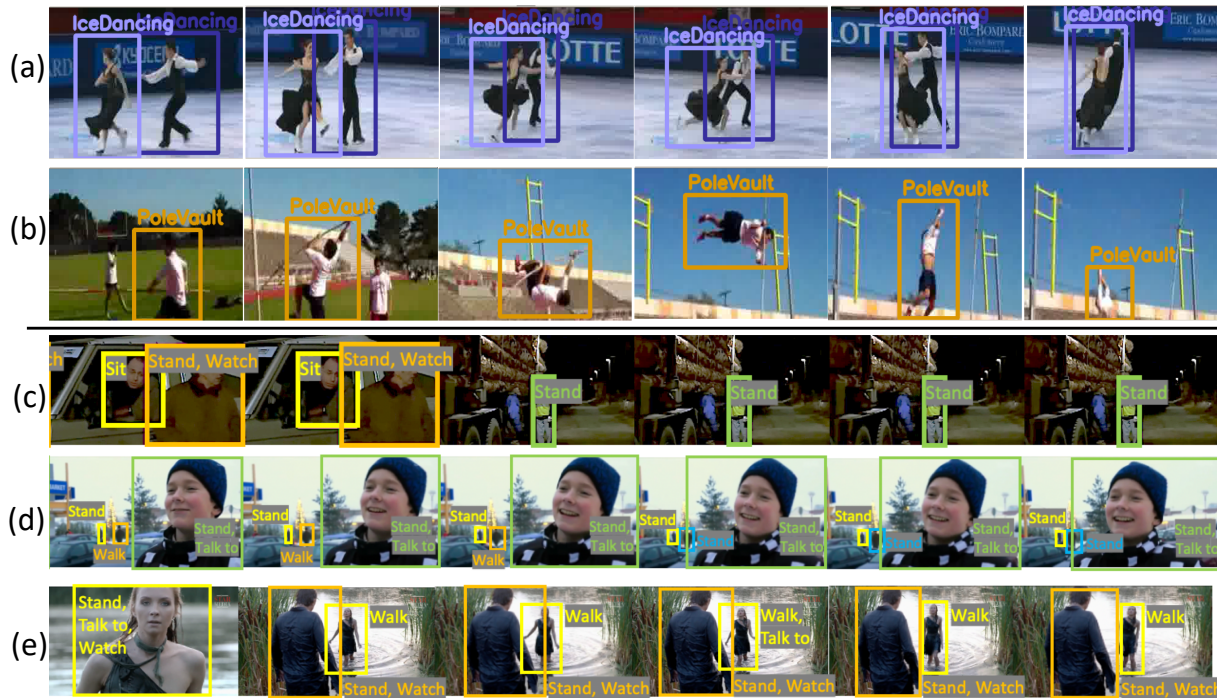
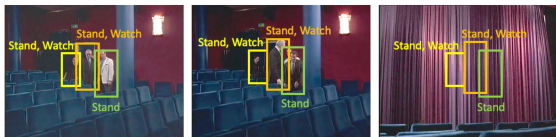


Figure 4: **Examples of action tubes** on UCF101-24 for clips with (a) multiple actors, (b) deformable actor; on AVA for clips with (c) scene change, (d) tiny actors. Each tube marked by a specific colour including its boxes and action labels. TubeR predicts precise action tubes with various lengths and aspect ratios. **Examples of actor tubes** on AVA(e). TubeR is able to generate precise actor tubes with linked bounding-boxes associated with the same person.

(a) Long band



(b) short band

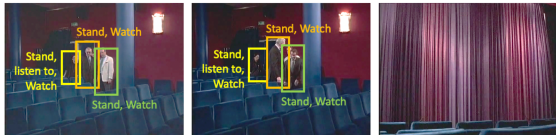


Figure 5: **Long band features vs. short band features** by multi-head attention layers. The short band features effectively relieve the false positive caused by scene cuts.

model may not generate precise temporal locations for some actors. Another way is decoding box queries from the corresponding frame features that we name *short band features*. As seen from the table, the short band features produce more precise action and actor detections. We show a challenging case with small actors and a scene cut in Figure 5. We observe the short band features effectively reduce the incorrect detection caused by scene cuts.

**Generalization ability.** In addition to the transformer part, the backbone for extracting video features also affects the final prediction. We consider various backbones for TubeR, including a single-branch I3D backbone and a two-

branch TPN [40] backbone for testing its generalization ability. All the backbones are pretrained on Kinetics-400. We report their action recognition accuracy on Kinetics-400. As shown in Table 6, adopting better pretrained models on action classification produces better action detection results. The proposed TubeR generalizes well on various backbones. Interestingly, we find that deeper networks based on Resnet101 present almost the same ability for detecting persons with the ones based on Resnet50, but the deeper networks improve action recognition.

**Error Analysis.** We compare the per-category *AP* of TubeR and a two-model method using SlowFastR101 on AVA. TubeR achieves better results on interactive actions, e.g. ‘drive’ +0.11, ‘play musical instrument’ +0.9 and, ‘work on a computer’ +0.4. TubeR is able to model the actor-object interaction while the two-model solution cannot do that (the bounding boxes used for ROI align only cover actors). We provide more analysis in the supplemental.

**Action tube visualization.** To visualize our action tube detection results, we show some challenging cases from UCF101-24 and AVA in Figure 4. In each clip, the detected tube is represented by its boxes with action labels, and different colors are used for different tubes. TubeR can detect multiple action tubes (a) and is also robust to deformations of actors (b). Moreover, TubeR handles the scene-cut case well (c). TubeR is also able to detect some tiny actions (d). (c-d)

show TubeR is capable of detecting action tubes with variable lengths. We also show an actor tube in (e). An actor tube generates a tube for an actor not action. Hence, the actions may change over time. An actor tube seems to track an actor and also tell the actions of the actor. We show more examples of action tubes and actor tubes in the supplementary.

## 5 Discussion

This paper proposes TubeR, the first transformer framework for video action tube detection. By learning a set of tube queries related to actions, TubeR does not require pre-defined anchors or a person detector. With the newly designed spatial→temporal multi-head self-attention layers, TubeR models actions in a spatio-temporal space and automatically generates their action tubes. TubeR outperforms well-developed one-model strategies and is close to two-model regimes, but more efficient during inference. We observe TubeR has potential on tracking an actor with different actions for long-range video understanding tasks, e.g. [23,35]. As TubeR performs detection and classification jointly, rather than separately, it converges slowly still. We believe speeding up training will reveal even more potential of transformers for video action detection, and beyond.

## References

- [1] Nicolas Carion, Francisco Massa, Gabriel Synnaeve, Nicolas Usunier, Alexander Kirillov, and Sergey Zagoruyko. End-to-end object detection with transformers. In *ECCV*, 2020. 1, 2, 5
- [2] Joao Carreira and Andrew Zisserman. Quo vadis, action recognition? a new model and the kinetics dataset. In *CVPR*, 2017. 2
- [3] Alexey Dosovitskiy, Lucas Beyer, Alexander Kolesnikov, Dirk Weissenborn, Xiaohua Zhai, Thomas Unterthiner, Mostafa Dehghani, Matthias Minderer, Georg Heigold, Sylvain Gelly, et al. An image is worth 16x16 words: Transformers for image recognition at scale. In *ICLR*, 2021. 1
- [4] Kaiwen Duan, Song Bai, Lingxi Xie, Honggang Qi, Qingming Huang, and Qi Tian. Centernet: Keypoint triplets for object detection. In *ICCV*, 2019. 2
- [5] Kevin Duarte, Yogesh Rawat, and Mubarak Shah. Videocapsulenet: A simplified network for action detection. In *NeurIPS*, 2018. 2
- [6] Christoph Feichtenhofer. X3d: Expanding architectures for efficient video recognition. In *CVPR*, 2020. 2, 6
- [7] Christoph Feichtenhofer, Haoqi Fan, Jitendra Malik, and Kaiming He. Slowfast networks for video recognition. In *CVPR*, 2019. 1, 2, 6, 7
- [8] Kirill Gavrilyuk, Ryan Sanford, Mehrsan Javan, and Cees GM Snoek. Actor-transformers for group activity recognition. In *CVPR*, 2020. 2
- [9] Rohit Girdhar, Joao Carreira, Carl Doersch, and Andrew Zisserman. A better baseline for ava. *arXiv preprint arXiv:1807.10066*, 2018. 1, 6
- [10] Rohit Girdhar, Joao Carreira, Carl Doersch, and Andrew Zisserman. Video action transformer network. In *CVPR*, 2019. 2, 6
- [11] Ross Girshick. Fast r-cnn. In *ICCV*, 2015. 1
- [12] Georgia Gkioxari and Jitendra Malik. Finding action tubes. In *CVPR*, 2015. 2
- [13] Chunhui Gu, Chen Sun, David A Ross, Carl Vondrick, Caroline Pantofaru, Yeqing Li, Sudheendra Vijayanarasimhan, George Toderici, Susanna Ricco, Rahul Sukthankar, et al. Ava: A video dataset of spatio-temporally localized atomic visual actions. In *CVPR*, 2018. 2, 5, 6
- [14] Rui Hou, Chen Chen, and Mubarak Shah. Tube convolutional neural network (t-cnn) for action detection in videos. In *ICCV*, 2017. 2
- [15] Hueihan Jhuang, Juergen Gall, Silvia Zuffi, Cordelia Schmid, and Michael J Black. Towards understanding action recognition. In *ICCV*, 2013. 5
- [16] Jianwen Jiang, Yu Cao, Lin Song, Shiwei Zhang Yunkai Li, Ziyao Xu, Qian Wu, Chuang Gan, Chi Zhang, and Gang Yu. Human centric spatio-temporal action localization. In *CVPRw*, 2018. 1, 2, 6
- [17] Vicky Kalogeiton, Philippe Weinzaepfel, Vittorio Ferrari, and Cordelia Schmid. Action tubelet detector for spatio-temporal action localization. In *ICCV*, 2017. 2, 6
- [18] Aisha Urooj Khan, Amir Mazaheri, Niels da Vitoria Lobo, and Mubarak Shah. Mmft-bert: Multimodal fusion transformer with bert encodings for visual question answering. *arXiv preprint arXiv:2010.14095*, 2020. 1
- [19] Harold W Kuhn. The hungarian method for the assignment problem. *Naval research logistics quarterly*, 1955. 5
- [20] Guang Li, Linchao Zhu, Ping Liu, and Yi Yang. Entangled transformer for image captioning. In *ICCV*, 2019. 1
- [21] Wei Li, Zehuan Yuan, Dashan Guo, Lei Huang, Xiangzhong Fang, and Changhu Wang. Deformable tube network for action detection in videos. *CVPR*, 2019. 2
- [22] Yixuan Li, Zixu Wang, Limin Wang, and Gangshan Wu. Actions as moving points. In *ECCV*, 2020. 2, 6
- [23] Chenchen Liu, Yang Jin, Kehan Xu, Guoqiang Gong, and Yadong Mu. Beyond short-term snippet: Video relation detection with spatio-temporal global context. In *CVPR*, 2020. 9
- [24] Ilya Loshchilov and Frank Hutter. Decoupled weight decay regularization. *ICLR*, 2017. 6
- [25] Xiaojiang Peng and Cordelia Schmid. Multi-region two-stream r-cnn for action detection. In *ECCV*, 2016. 2
- [26] Rizard Renanda Adhi Pramono, Yie-Tarng Chen, and Wen-Hsien Fang. Hierarchical self-attention network for action localization in videos. In *ICCV*, 2019. 2
- [27] Shaoqing Ren, Kaiming He, Ross Girshick, and Jian Sun. Faster r-cnn: Towards real-time object detection with region proposal networks. In *NIPS*, 2015. 4
- [28] Hamid Rezaatofghi, Nathan Tsoi, JunYoung Gwak, Amir Sadeghian, Ian Reid, and Silvio Savarese. Generalized intersection over union: A metric and a loss for bounding box regression. In *CVPR*, 2019. 5

- [29] Gurkirt Singh, Suman Saha, Michael Sapienza, Philip HS Torr, and Fabio Cuzzolin. Online real-time multiple spatiotemporal action localisation and prediction. In *ICCV*, 2017. 1, 2, 5
- [30] Lin Song, Shiwei Zhang, Gang Yu, and Hongbin Sun. Tacnet: Transition-aware context network for spatio-temporal action detection. In *CVPR*, 2019. 6
- [31] Khurram Soomro, Amir Roshan Zamir, and Mubarak Shah. Ucf101: A dataset of 101 human actions classes from videos in the wild. *arXiv preprint arXiv:1212.0402*, 2012. 5
- [32] Russell Stewart, Mykhaylo Andriluka, and Andrew Y Ng. End-to-end people detection in crowded scenes. In *CVPR*, 2016. 5
- [33] Chen Sun, Abhinav Shrivastava, Carl Vondrick, Kevin Murphy, Rahul Sukthankar, and Cordelia Schmid. Actor-centric relation network. In *ECCV*, 2018. 1, 2, 6
- [34] Chiranjib Sur. Self-segregating and coordinated-segregating transformer for focused deep multi-modular network for visual question answering. *arXiv preprint arXiv:2006.14264*, 2020. 1
- [35] Yao-Hung Hubert Tsai, Santosh Divvala, Louis-Philippe Morency, Ruslan Salakhutdinov, and Ali Farhadi. Video relationship reasoning using gated spatio-temporal energy graph. In *CVPR*, 2019. 9
- [36] Ashish Vaswani, Noam Shazeer, Niki Parmar, Jakob Uszkoreit, Llion Jones, Aidan N Gomez, Łukasz Kaiser, and Illia Polosukhin. Attention is all you need. In *NIPS*, 2017. 1, 3
- [37] Philippe Weinzaepfel, Zaid Harchaoui, and Cordelia Schmid. Learning to track for spatio-temporal action localization. In *ICCV*, 2015. 2
- [38] Chao-Yuan Wu, Christoph Feichtenhofer, Haoqi Fan, Kaiming He, Philipp Krahenbuhl, and Ross Girshick. Long-term feature banks for detailed video understanding. In *CVPR*, 2019. 2
- [39] Saining Xie, Chen Sun, Jonathan Huang, Zhuowen Tu, and Kevin Murphy. Rethinking spatiotemporal feature learning: Speed-accuracy trade-offs in video classification. In *ECCV*, 2018. 2
- [40] Ceyuan Yang, Yinghao Xu, Jianping Shi, Bo Dai, and Bolei Zhou. Temporal pyramid network for action recognition. In *CVPR*, 2020. 6, 7, 8
- [41] Xitong Yang, Xiaodong Yang, Ming-Yu Liu, Fanyi Xiao, Larry S Davis, and Jan Kautz. Step: Spatio-temporal progressive learning for video action detection. In *CVPR*, 2019. 1, 2, 6
- [42] Yuancheng Ye, Xiaodong Yang, and Yingli Tian. Discovering spatio-temporal action tubes. *JVCIR*, 58:515–524, 2019. 2
- [43] Li Yuan, Yunpeng Chen, Tao Wang, Weihao Yu, Yujun Shi, Francis EH Tay, Jiashi Feng, and Shuicheng Yan. Tokens-to-token vit: Training vision transformers from scratch on imagenet. *arXiv preprint arXiv:2101.11986*, 2021. 1
- [44] Yubo Zhang, Pavel Tokmakov, Martial Hebert, and Cordelia Schmid. A structured model for action detection. In *CVPR*, 2019. 2
- [45] Jiaojiao Zhao and Cees GM Snoek. Dance with flow: Two-in-one stream action detection. In *CVPR*, 2019. 2, 6
- [46] Xizhou Zhu, Weijie Su, Lewei Lu, Bin Li, Xiaogang Wang, and Jifeng Dai. Deformable DETR: Deformable transformers for end-to-end object detection. In *ICLR*, 2021. 1, 2